AGU PUBLICATIONS

JGR

Journal of Geophysical Research: Atmospheres

RESEARCH ARTICLE
10.1002/2016JD025606

Key Points:
- The recent warming in Spitsbergen is mainly linked to changes in air mass characteristics and not to changes in atmospheric circulation
- Changes in air mass characteristics are associated with sea ice decline east and north of Spitsbergen, especially in winter
- Six atmospheric circulation types (out of 21) contribute approximately 80% of the recent warming

Correspondence to:
K. Isaksen,
ketili@met.no

Citation:
Isaksen, K., Ø. Nordli, E. J. Førland, E. Łupikasza, S. Eastwood, and T. Niedźwiedź (2016), Recent warming on Spitsbergen—Influence of atmospheric circulation and sea ice cover, *J. Geophys. Res. Atmos.*, *121*, 11,913–11,931, doi:10.1002/2016JD025606.

Received 1 JUL 2016
Accepted 20 SEP 2016
Accepted article online 24 SEP 2016
Published online 18 OCT 2016

Recent warming on Spitsbergen—Influence of atmospheric circulation and sea ice cover

K. Isaksen[1], Ø. Nordli[1], E. J. Førland[2], E. Łupikasza[3], S. Eastwood[1], and T. Niedźwiedź[3]

[1]Department of Research and Development, Norwegian Meteorological Institute, Oslo, Norway, [2]Department of Observation and Climate, Norwegian Meteorological Institute, Oslo, Norway, [3]Department of Climatology, Faculty of Earth Sciences, University of Silesia, Katowice, Poland

Abstract Spitsbergen has experienced some of the most severe temperature changes in the Arctic during the last three decades. This study relates the recent warming to variations in large-scale atmospheric circulation (AC), air mass characteristics, and sea ice concentration (SIC), both regionally around Spitsbergen and locally in three fjords. We find substantial warming for all AC patterns for all seasons, with greatest temperature increase in winter. A major part of the warming can be attributed to changes in air mass characteristics associated with situations of both cyclonic and anticyclonic air advection from north and east and situations with a nonadvectional anticyclonic ridge. In total, six specific AC types (out of 21), which occur on average 41% of days in a year, contribute approximately 80% of the recent warming. The relationship between the land-based surface air temperature (SAT) and local and regional SIC was highly significant, particularly for the most contributing AC types. The high correlation between SAT and SIC for air masses from east and north of Spitsbergen suggests that a major part of the atmospheric warming observed in Spitsbergen is driven by heat exchange from the larger open water area in the Barents Sea and region north of Spitsbergen. Finally, our results show that changes in frequencies of AC play a minor role to the total recent surface warming. Thus, the strong warming in Spitsbergen in the latest decades is not driven by increased frequencies of "warm" AC types but rather from sea ice decline, higher sea surface temperatures, and a general background warming.

1. Introduction

The recent increase in annual temperatures over the Arctic is twice as fast as the global average [e.g., *Arctic Monitoring and Assessment Programme*, 2012; *Cohen et al.*, 2014; *Gjelten et al.*, 2016]. This "Arctic amplification" is due to a combination of a general background warming [e.g., *Fyfe et al.*, 2013], anomalies in the atmospheric circulation (AC) [e.g., *Overland and Serreze*, 2012; *Overland and Wang*, 2016], reduced sea ice extent and higher sea surface temperatures (SSTs) [e.g., *Serreze et al.*, 2011], increased water vapor [*Park et al.*, 2015] in addition to strong low-level stability, and cloud conditions [*Graversen et al.*, 2014; *Pithan and Mauritsen*, 2014].

During the recent warm period, from the beginning of the 21st century, Arctic-wide warm surface air temperature (SAT) anomalies have persisted and are associated with their own characteristic pressure patterns [*Overland et al.*, 2008]. Several studies [e.g., *Overland and Wang*, 2010; *Overland et al.*, 2011, 2012] suggest that the recent loss of Arctic sea ice is the main contributor for the high Arctic SATs during these later years, not only by directly altering the heat budget of the atmosphere in the area but also by causing modification of large-scale AC [*Jaiser et al.*, 2012]. However, a recent study by *Navarro et al.* [2016] shows that sulfate aerosol reductions in Europe since 1980 can potentially explain a significant fraction of Arctic warming over that period.

The Svalbard archipelago (74°–81°N, 10°–35°E; see Figure 1) is one of the northernmost land areas in the Arctic Ocean and is among the regions that has experienced the greatest temperature increase during the last three decades [*Nordli et al.*, 2014]. While the dynamics of the warming in Svalbard prior to the 1930s is still not fully understood, the warming from the 1960s to the mid-1990s is clearly linked to variations in AC [*Hanssen-Bauer and Førland*, 1998]. The recent period (from the beginning of the 21st century), however, shows a rather different pattern. While 6 of the 10 warmest winters in the Svalbard Airport composite series 1898 to present [*Nordli et al.*, 2014] occurred after 2000 (2005–2007, 2010, 2012, and 2014), several of these winters were characterized by average or even low Arctic Oscillation (AO) mode. This indicates that there are other, more regional, sea level pressure (SLP) patterns that may contribute significantly to interannual variability in sea ice extent and SAT [cf. *Maslanik et al.*, 2007].

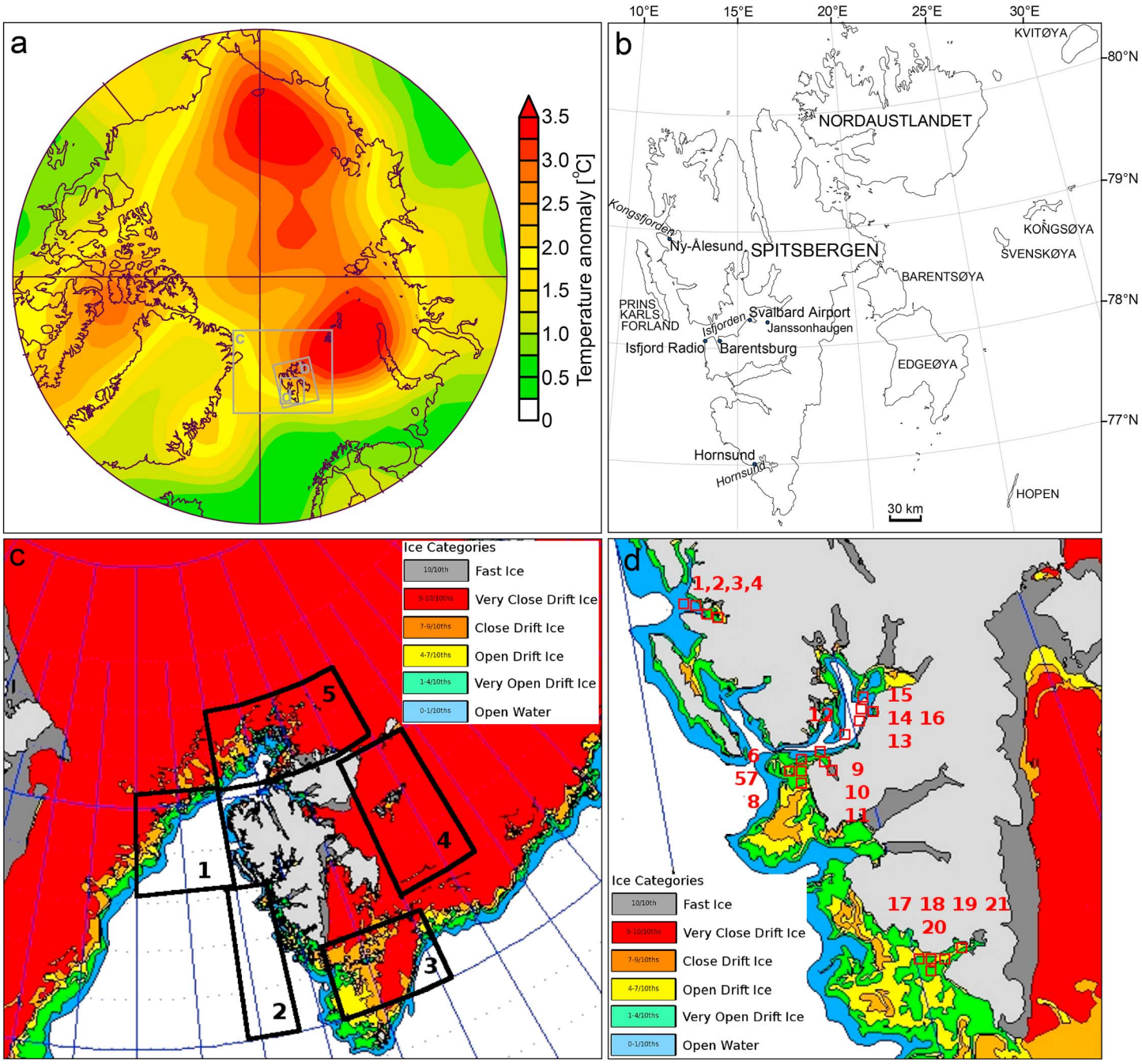

Figure 1. (a) Average air temperature anomalies during 2001–2015 (with respect to the 1971–2000 mean) across the Arctic from the NCEP Reanalysis [*Kalnay et al.*, 1996]. (b–d) Study areas are marked by boxes. Data provided by the NOAA/Earth System Research Laboratory (ESRL) Physical Sciences Division, Boulder, Colorado (www.esrl.noaa.gov/psd/). Figure 1b shows location of meteorological stations on Spitsbergen used in this study. Figure 1c shows example of map of regional sea ice concentration (SIC) (14 March 2013) and five geographical areas lying NW (1), SW (2), SE (3), E (4), and N (5) in respect to Spitsbergen. Figure 1d shows map of SIC in the fjords on western Spitsbergen (same date as in Figure 1c). The numbers refer to SIC locations/points used in local analysis. Data are provided by Istjenesten, MET Norway, http://polarview.met.no/.

The rapid Arctic warming has contributed to dramatic melting of Arctic sea ice and spring snow cover, at a pace greater than that simulated by climate models [*Cohen et al.*, 2014]. However, not only the reduction of the sea ice cover around Svalbard [e.g., *Onarheim et al.*, 2014] but also the reduction in fjord ice cover [e.g., *Muckenhuber et al.*, 2016] have considerable impact on all components of local climate in the fjords. All key meteorological stations with long climate series at Svalbard are situated in the fjords on western

Spitsbergen, which is the largest island in Svalbard (Figure 1). Therefore, the climate records are disproportionally sensitive to changes of both the sea ice cover around Svalbard and the local fjord ice cover.

Several studies have addressed trends and variability in SAT within the Svalbard region [e.g., *Førland et al*., 1997; *Hanssen-Bauer*, 2002; *Niedźwiedź*, 2003; *Przybylak*, 2007; *Førland et al*., 2011; *Marsz and Styszynska*, 2013; *Lupikasza and Niedźwiedź*, 2013; *Lupikasza et al*., 2014; *Nordli et al*., 2014; *Gjelten et al*., 2016] and variations in sea ice coverage [e.g., *Deser et al*., 2000; *Kwok and Rothrock*, 2009; *Lindsay et al*., 2009; *Onarheim et al*., 2014; *Muckenhuber et al*., 2016]. The present analysis combines and extends these earlier studies by quantitatively relating the recent warming on Spitsbergen to large-scale AC and sea ice concentration (SIC) variations. Moreover, information on SIC in the fjords has been applied to study the influence of ice-covered waters on local SATs.

This study examines the recent SAT anomalies on western Spitsbergen and their relation to AC and SIC. Specifically, we address the following three research questions (RQs):

How much of the recent warming is caused by changes in AC?
How much of the recent warming is caused by changes in air mass characteristics?
What is the influence on recent warming of changes in feedback effects caused by reduced SIC?

To elucidate these questions, we use daily SAT measurements from six meteorological stations along the coast and fjords of western Spitsbergen (Figure 1). These temperature series have recently been digitized and quality controlled in a Norwegian, Russian, and Polish collaboration [*Gjelten et al*., 2016]. Further, a data set of daily AC classification over Spitsbergen is used [*Niedźwiedź*, 1993]. Finally, daily to weekly high-resolution SIC data are used both for local and regional analyses to study the influence of SIC on SAT in the fjords and the sea area around the islands.

2. Data and Methods

2.1. Surface Air Temperature (SAT)

Long-term, daily SAT series from the stations Hornsund, Isfjord Radio, Barentsburg, Svalbard Airport, and Ny-Ålesund (Figure 1b) were recently scrutinized and homogenized [*Gjelten et al*., 2016]. The five stations are all situated close to the fjords (Isfjorden, Hornsund, and Kongsfjorden; see Figure 1b) and coast at elevations between 7 and 28 m above sea level (asl), except Barentsburg which is located 74 m asl.

The stations Hornsund, Isfjord Radio, and Ny-Ålesund constitute a coastal south-north transect, while the stations Isfjord Radio, Barentsburg, and Svalbard Airport are located in a west-east transect along Isfjorden. Isfjord Radio, located at the mouth of the Isfjorden system, is influenced by Atlantic water (AW) from the West Spitsbergen Shelf year round. In contrast, the entrance to Isfjorden, which corresponds to the location of Barentsburg, demarcates the more eastern, inshore part of the fjord that is influenced by AW seasonally [*Nilsen et al*., 2008]. Svalbard Airport is the most "continental" station, lying in central parts of Isfjorden, 49 km NE to Isfjord Radio (Figure 1b).

To support analyses related to how the SIC in Isfjorden affects local SAT at Svalbard Airport, we included a station located in Adventdalen at Janssonhaugen [*Isaksen et al*., 2007] at a higher elevation (270 m asl) and away from the fjord. The data series at Janssonhaugen start in 2000.

2.2. Atmospheric Circulation (AC) Classification

The calendar of AC types ("Niedźwiedź Classification") [*Niedźwiedź*, 2013] was created manually based on German synoptic maps published in "Tägliche Wetterbericht" (1950–1975), "Europäischer Wetterbericht" (1976–2000), and after 2000 on the DWD Archives (http://www.wetter3.de/Archiv/archiv_dwd.html). It consists of 21 AC types denoted by capital letters that show the direction of air advection (e.g., N = northern, NE = northeastern) and small letters that show the type of pressure system (a = anticyclone, c = cyclone). Every day since December 1950 has been attributed to one of the 21 AC types. The air advection corresponds to geostrophic wind direction assessed using the pattern of SLP. In addition to 16 types with distinct air advection, the calendar includes four nonadvectional types (Ca = anticyclonic centre over or very near Spitsbergen, Ka = anticyclonic ridge, Cc = center of cyclone over or very near Spitsbergen, Bc = cyclonic trough) and one unclassified type x. The classification is methodologically similar to the well-known *Lamb* [1972] classification for the British Isles.

2.3. Temperature Change Due to Changes in AC and Air Mass Characteristics

The period 1971–2000 is recommended as the normal period for present climate [*World Meteorological Organization*, 2011]. In the present study the latest period 2001–2015 is compared with this normal. Temperature anomaly, T_C, due to changed AC in the period 2001–2015 compared to the normal period, 1971–2000, was calculated by formula (1), and temperature anomaly, T_d, due to changes in air mass characteristics in the period 2001–2015 compared to the normal period, 1971–2000, was calculated by formula (2)

$$T_c = \sum_{i=1}^{n} (f_{1i} - f_{0i}) T_{0i} \quad (1)$$

$$T_d = \sum_{i=1}^{n} (T_{1i} - T_{0i}) f_{0i} \quad (2)$$

where f_{1i} and f_{0i} are the frequency of AC type i in the period 2001–2015 and 1971–2000, respectively. T_{1i} and T_{0i} is the mean temperature for AC type i during the period 2001–2015 and 1971–2000, respectively, whereas n is the total number of AC types.

2.4. Sea Ice Concentration (SIC) Data

SIC data were based on two sources.

1. The European Organisation for the Exploitation of Meteorological Satellites (EUMETSAT) Ocean and Sea Ice Satellite Application Facility (OSI SAF, http://osisaf.met.no/) has reprocessed the time series of passive microwave satellite data from 1979 to 2015 and produced a data record of daily SIC [*Tonboe et al*., 2016]. These passive microwave data have low resolution, but global coverage, and can be used to calculate SIC during all weather conditions. The OSI SAF processing has been done with a dynamical algorithm to deal with changing satellite instruments and seasonal variations and hence ensure a climate-consistent data record. Due to the low resolution of the satellite data (~50 km), this data record cannot be used in detailed studies close to the coastline.

The OSI SAF data record was used to study interactions between SIC and SAT on a regional scale. Daily average SIC was calculated for the period 1979–2015 for five selected regions around Spitsbergen (Figure 1c). The influence on SAT by SIC in the different ice regions was tested by stepwise regression analysis with SAT as predictand and regional SIC as predictors. SIC from all five regions was accepted as potential predictors, but significance tests decided which regions were accepted as predictors in the final model. The number of predictors in the final model varied from one to five for the various seasons and AC types. Each SIC observation was related to the actual AC type.

2. Ice charts have been produced routinely by the Norwegian Ice Service (NIS, http://met.no/English/Ocean_and_Ice/) since the winter of 1969/1970. In the beginning the charts were based on analogue infrared satellite images but since the summer of 2007 increasing volumes of high-resolution synthetic aperture radar satellite data have become available. More details are found in *Hughes and Wagner* [2015].

The NIS data set has been used to study interactions between SIC and SAT at a local scale in the fjords Hornsund, Isfjorden, and Kongsfjorden for the period 1975–2015. Time series were produced based on 21 predefined points (see Figure 1d) that were located near the meteorological stations Ny-Ålesund (points 1–4), Isfjord Radio (5–8), Barentsburg (9–11), Svalbard Airport (13–16), and Hornsund (17–21). Analyses showed that the SIC at certain data points had no particular influence on SAT compared to their neighbors, so we used the average SIC for the points 3–5 near each station. Thus, one ice data series was defined as the local SIC related to each meteorological station.

3. Results

3.1. Temperature Normals and Recent Anomalies

Table 1 shows that the average annual temperature in the normal period 1971–2000 ranges from −4.4°C for Isfjord Radio to −5.9°C at Svalbard Airport and with average winter temperatures of −10.7 to −13.9°C, respectively. Monthly average temperatures (Figure 2a) demonstrate the local temperature gradients from Hornsund in the south to Ny-Ålesund in the north along the coast of western Spitsbergen. The northern part of Spitsbergen is coldest in winter, spring, and autumn. In summer, however, Hornsund in the south is the coldest station [cf. *Gjelten et al*., 2016]. This is related to the Sørkapp Current that carries cold and less saline waters from the Barents Sea around the southern Spitsbergen tip and isolates Hornsund from the warm AW

Table 1. Mean Temperatures for the Normal Period 1971–2000 and Temperature Change From 1971–2000 to 2001–2015

	Mean Temperature 1971–2000 (°C)					Temperature Change From 1971–2000 to 2001–2015 (°C)				
Station	Annual	Winter	Spring	Summer	Autumn	Annual	Winter	Spring	Summer	Autumn
Hornsund	−4.7	−11.2	−7.7	3.3	−3.2	1.9	4.0	1.4	0.7	1.7
Isfjord Radio	−4.4	−10.7	−7.7	4.0	−3.1	1.7	3.4	1.5	0.7	1.2
Barentsburg	−5.5	−12.7	−9.1	4.1	−4.2	1.9	3.8	1.8	0.9	1.3
Svalbard Ap.	−5.9	−13.9	−9.6	4.5	−4.7	2.5	4.6	2.1	1.4	1.9
Ny-Ålesund	−5.7	−12.9	−8.8	3.7	−4.7	1.8	3.8	1.4	0.8	1.2

[*Walczowski*, 2013]. Weather stations located farther to the north are more influenced by heat exchange from the AW. The figure also demonstrates the gradient from the outer western and maritime Isfjord Radio to the more continental Svalbard Airport, the latter being the coldest station in winter, spring, and autumn, while it is the warmest in summer [cf. *Gjelten et al*., 2016].

From the normal period 1971–2000 to the most recent 15 year period 2001–2015, the station-wise increase in average annual temperatures is between 1.7 and 2.5°C (Table 1). The temperature has increased in all seasons with the strongest increase in winter months. The average winter temperatures have increased by 3.4–4.6°C, while the summer increases at all stations are between 0.7 and 1.4°C.

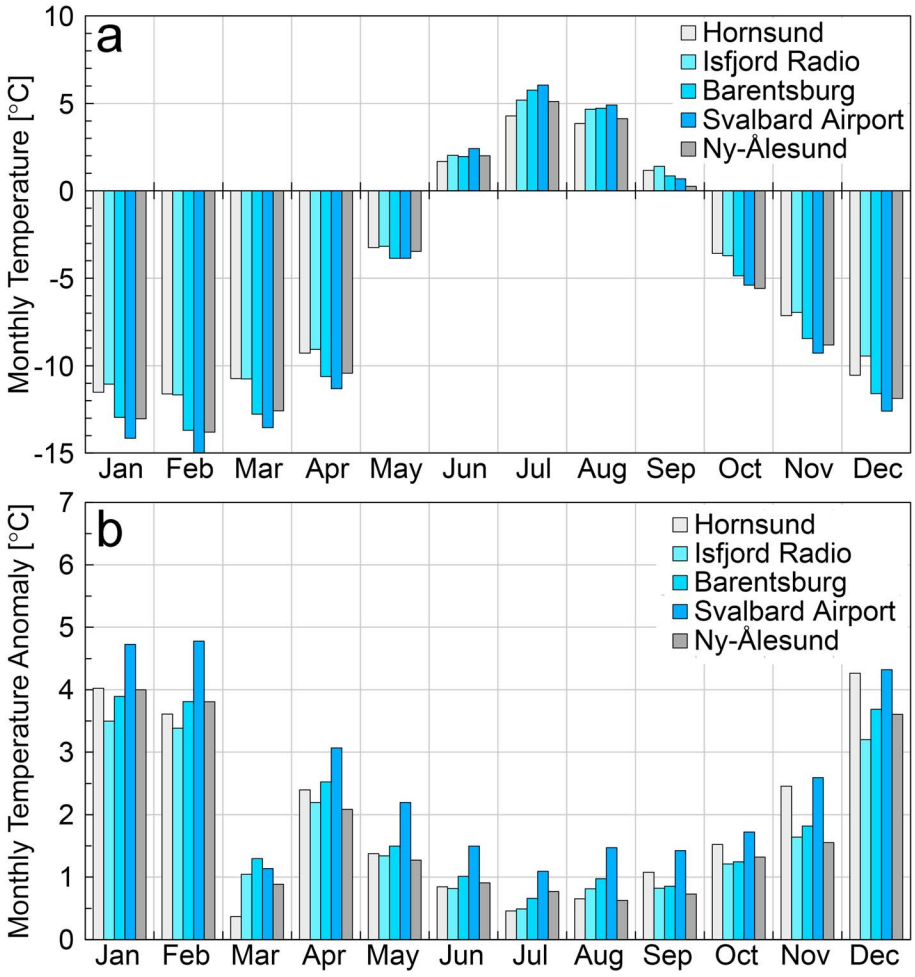

Figure 2. (a) Average monthly air temperature (°C) during the normal period 1971–2000. (b) Average monthly air temperature anomalies during the recent period 2001–2015 (with respect to the 1971–2000 mean). Weather stations are ordered from south (Hornsund, light grey) to north (Ny-Ålesund, dark grey) and from west to east, from the mouth area of Isfjorden (Isfjord Radio, light blue) toward the entrance to Isfjorden (Barentsburg, medium light blue) and central parts of Isfjorden (Svalbard Airport, dark blue).

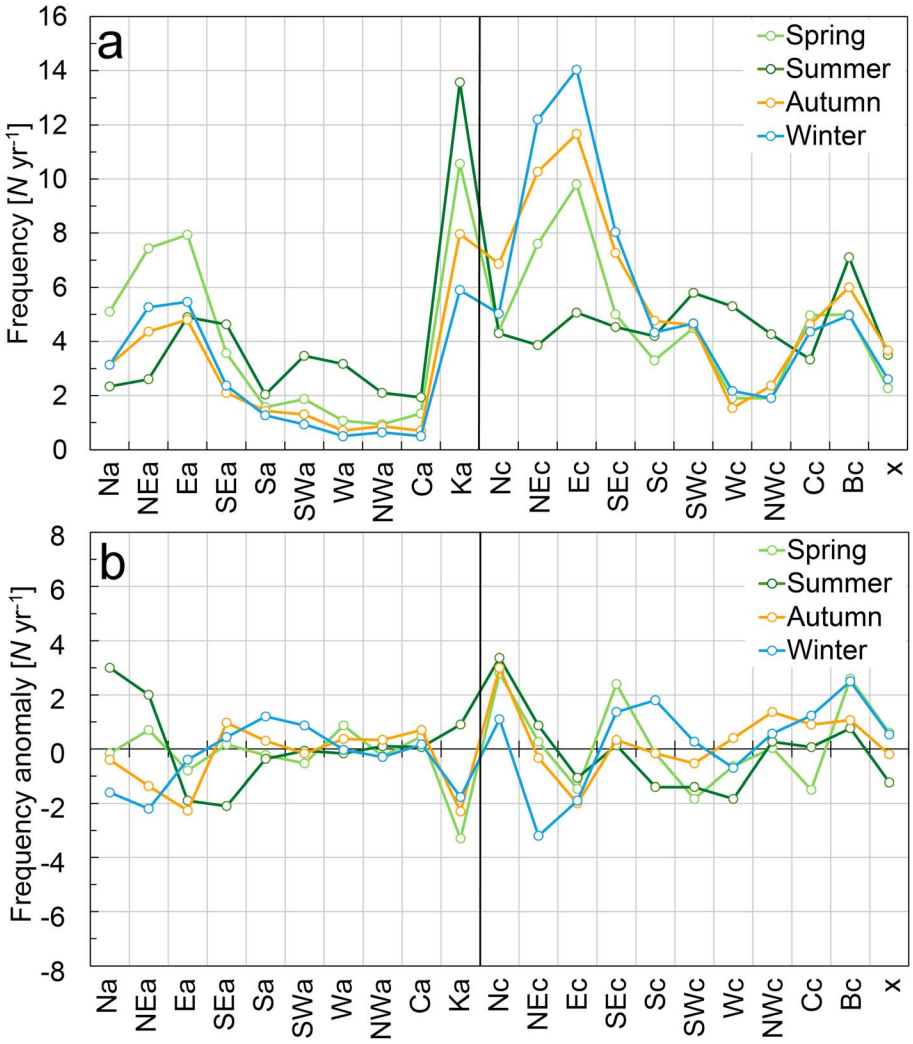

Figure 3. (a) Average seasonal frequency ($N\,yr^{-1}$) of atmospheric circulation (AC) types during the normal period 1971–2000. (b) Average seasonal frequency anomalies during the recent period 2001–2015 (with respect to the 1971–2000 mean). For explanation of AC types (*x* axis); see section 2.2.

On a monthly scale, March shows less temperature increase compared to the winter months and also compared to April and May. In general, there is a similar pattern for all stations (Figure 2b). Svalbard Airport shows the greatest temperature increase except in March. The south-north gradient along western Spitsbergen, however, is not so clear, e.g., for October to December and for 5 months during spring, summer, and autumn, Hornsund shows nearly the same temperature anomalies as Svalbard Airport. For 5 months Ny-Ålesund has the lowest-temperature anomalies among the stations.

3.2. Frequency of Atmospheric Circulation (AC) Types

The most intense cyclonic activity is in winter. The main feature of the SLP distribution in winter is a vast trough stretching from the Icelandic Low throughout the Norwegian Sea and Barents Sea. Located in the northern part of that trough, Spitsbergen experiences an inflow of air from the eastern sector. In spring cyclonic activity weakens and Spitsbergen becomes influenced by the Greenland High [*Niedźwiedź*, 2013]. In summer the AC is often dominated by small horizontal pressure gradients until the end of August [*Niedźwiedź*, 2013]. *Brümmer et al*. [2000] suggest that in summer the cyclonic activity is even higher than in winter, but these summer cyclones are much shallower and less intense than those in winter.

In Figure 3a average seasonal frequency of AC types during the normal period 1971–2000 is shown. In summer the frequencies are relatively evenly distributed among all AC types. Summer has also the lowest

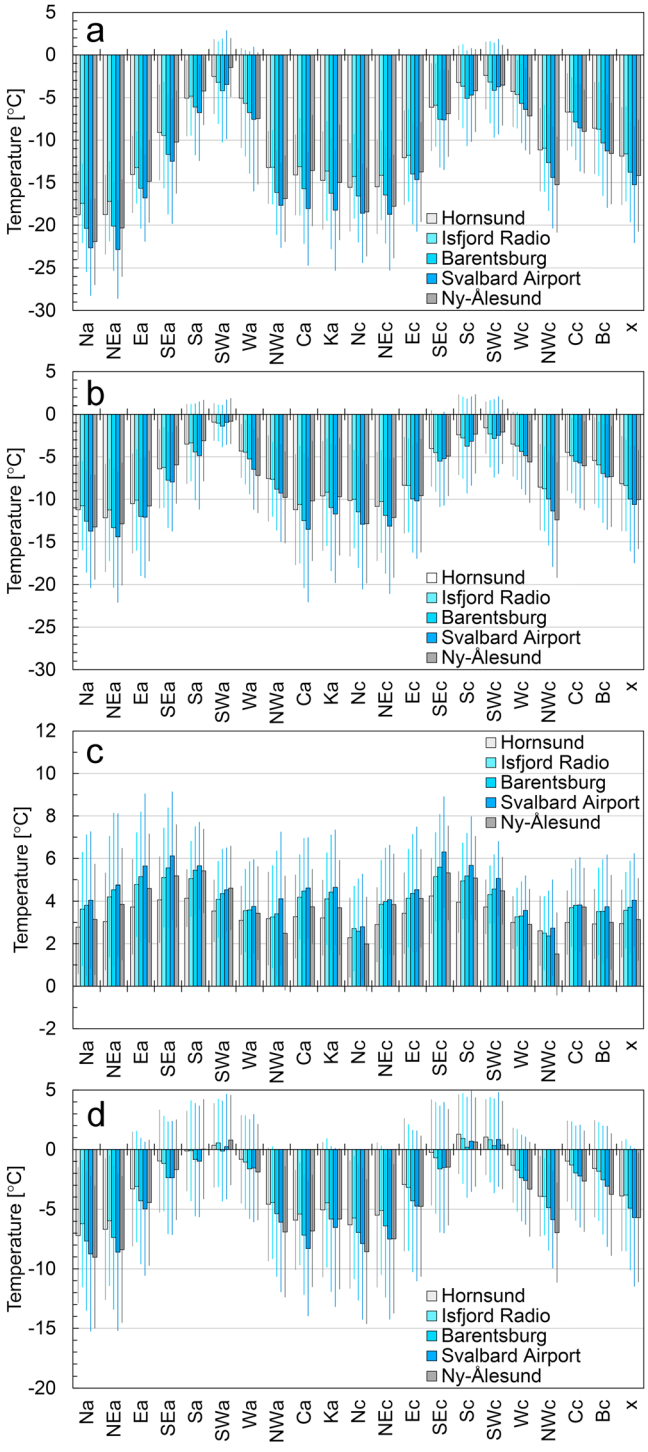

Figure 4. Average daily air temperatures during the normal period 1971–2000 for the various AC types over (a) winter, (b) spring, (c) summer, and (d) autumn. Error bars represent one standard deviation.

frequency of cyclonic types particularly for air advection from the eastern sector. However, the highest frequency of the nonadvectional anticyclonic ridge (Ka) type occurs during summer. Ka is also the most frequent type in spring followed by northeasterly to easterly (NE-E) flow during both cyclonic (c) and anticyclonic (a) AC. Also, in autumn NE-E cyclonic flow is most frequent, followed by cyclonic trough (Bc). In winter, NE-SE cyclonic flow dominates, followed by anticyclonic ridge (Ka) and NE-E anticyclonic flow.

Figure 3b shows the average seasonal frequency anomalies during the recent period 2001–2015 (with respect to the 1971–2000 mean). For most AC types anomalies are, in general, less than $\pm 2\,\mathrm{N\,yr^{-1}}$. However, regarding the most frequent types (cf. Figure 3a) negative anomalies for Ka are evident during spring, autumn, and winter (Figure 3b). During winter the frequency of NEc-Ec flow and Na-NEa flow, bringing cold air from the center of the Arctic, is becoming less frequent for the recent 2001–2015 period. In contrast, air advection from the southern sector, bringing moist and warm air, is slightly more frequent. For frequent AC types in spring and autumn negative anomalies are associated with Ec flow.

3.3. Surface Air Temperature (SAT) During Different Atmospheric Circulation (AC) Types

Air masses flowing over Spitsbergen display a variety of thermal properties. Figure 4 clearly shows that the air temperature to a large extent is governed by the direction of air advection. In every season the lowest air temperatures are related to air advection from the northern and northeastern directions. This is particularly the case under anticyclonic AC when the weather is dominated by stable thermal conditions and cloud formation normally is constrained. Low temperatures are also found for the nonadvectional anticyclonic types Ka and Ca, with low wind speeds and potential for local temperature inversions. In contrast, the highest temperatures are associated with air flow from southern sector, during both cyclonic and anticyclonic conditions. With southerly flow, the climate at Spitsbergen is mild even in winter, with mean

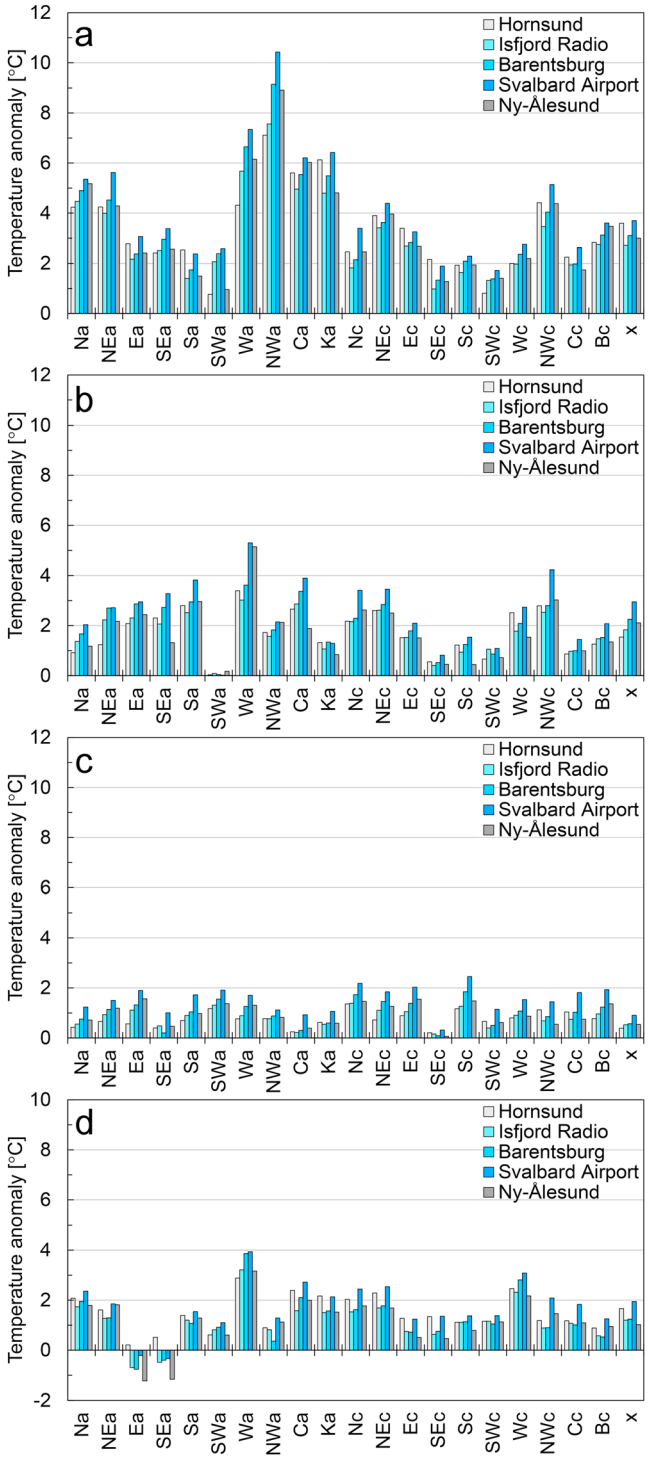

Figure 5. Average air temperature anomalies during the recent period 2001–2015 (with respect to the 1971–2000 mean) for the various AC types over (a) winter, (b) spring, (c) summer, and (d) autumn.

temperatures a few degrees below 0°C for all stations. For instance, at Svalbard Airport, the largest difference in mean daily temperatures occurs between the types NEa (−23°C) and SWa (−4°C) in winter. The standard deviations shown in Figure 4 highlight the wide range of daily temperatures that occur for every AC type, particularly in winter, spring, and autumn.

The temperature differences between the weather stations seem not to vary much with respect to the AC types. However, during summer the northern station Ny-Ålesund seems to be relatively colder compared to the other stations for AC types Wc and NWc. Such AC types are bringing colder air from the Greenland Sea and Arctic Ocean, especially over northern Spitsbergen.

3.4. Temperature Anomalies in Relation to Atmospheric Circulation (AC) Types

Seasonal changes in average air temperature from 1971–2000 to 2001–2015 for the various AC types are shown in Figure 5. Except for Ea and SEa during autumn, all AC types indicate higher temperatures for the recent period. The most striking anomalies are seen during winter for anticyclonic flow from NW and W, followed by the two non-advectional types Ca and Ka. For anticyclonic flow from NW, the mean temperature at Svalbard Airport is 10°C higher for the recent period 2001–2015 than during 1971–2000.

However, as shown in Figure 3b the seasonal frequency of some AC types is very rare (only a few days/year for some types). Particularly, the AC types with largest anomalies (NWa and Wa) rarely occur and the confidence intervals of the mean values are large. Thus, due to the great differences in frequencies, a biased impression of anomalies is apparently shown in Figure 5.

To fully capture which of the AC patterns that are contributing most to the recent temperature increase, the frequency must be included. In Figure 6 the cumulative air temperature anomalies associated with the various AC types over the different seasons are shown. The greatest contribution to the recent warming is associated with situations of cyclonic air advection from northeast-east (NEc and Ec), anticyclonic air advection

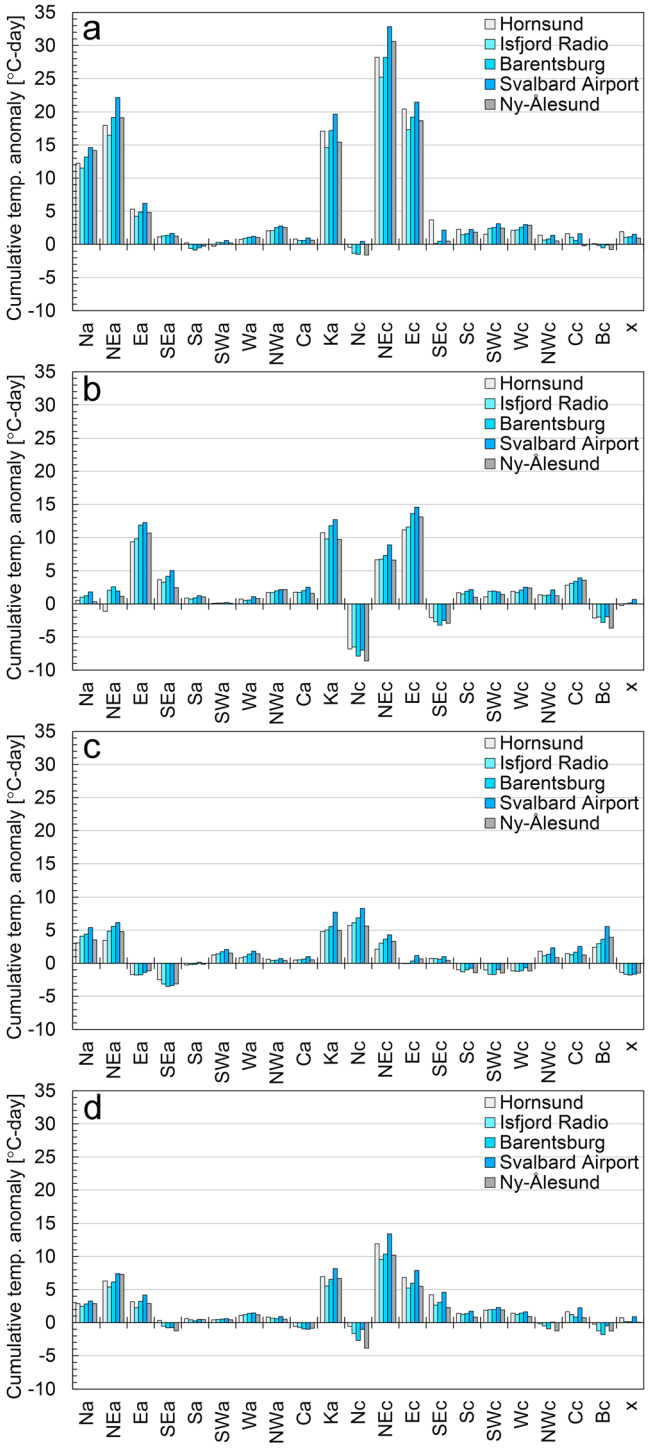

Figure 6. Cumulative air temperature anomalies during the recent period 2001–2015 (with respect to the 1971–2000 mean) within the various AC types over (a) winter, (b) spring, (c) summer, and (d) autumn.

from northeast (Na, NEa, and Ea), and situations with anticyclonic ridge (Ka). These six types contribute in total approximately 80% of the recent warming.

The monthly temperature anomalies for these six types are shown in Figure 7. The annual amplitude of these anomalies increases, from the lowest for the two eastern advection types (Ec and Ea) to the greatest for the northern advection types (Na, NEa, and NEc) and anticyclonic ridge (Ka) type. Greatest warming is seen in February. The smallest monthly anomalies are found for the period April to September. The only negative anomaly is for October during Ea type.

Figure 8 shows an example of typical SLP pattern over Svalbard for these types. The type Na (occurring 4.0% of days during 2001–2015) is linked to a well-developed anticyclone with its center located over the eastern part of Greenland which causes the air to flow from the central part of the Arctic Ocean. Similar conditions are induced by an anticyclone located between north Greenland and the Pole, but with air advection from the northeast (NEa, 5.1%). The AC-type Ea (6.9%) is usually linked to high pressure centered northeast of Spitsbergen where the air masses have their origins over the Siberian Arctic and reach Spitsbergen on an easterly air stream. The thermal characteristic of these air masses changes throughout the year—they are cold in winter and warm in summer. The nonadvective anticyclonic ridge type (Ka, 8.6%) with a prominent descent of the air enhances the impact of local conditions on air temperature. The NEc type (8.6%) is related to low-pressure systems moving from over Norway and deep into the Barents Sea, reaching Novaya Zemlya and brings colder air from the Arctic Ocean over Spitsbergen. The most frequent AC on an annual scale, Ec (9.3%), is similar to the previous case but with the only distinction that the low does not penetrate so deeply into the Barents Sea. During winter and spring NEc and especially Ec bring warmer air masses compared to the three anticyclone types, sourced from the northern part of the Atlantic Ocean and Europe.

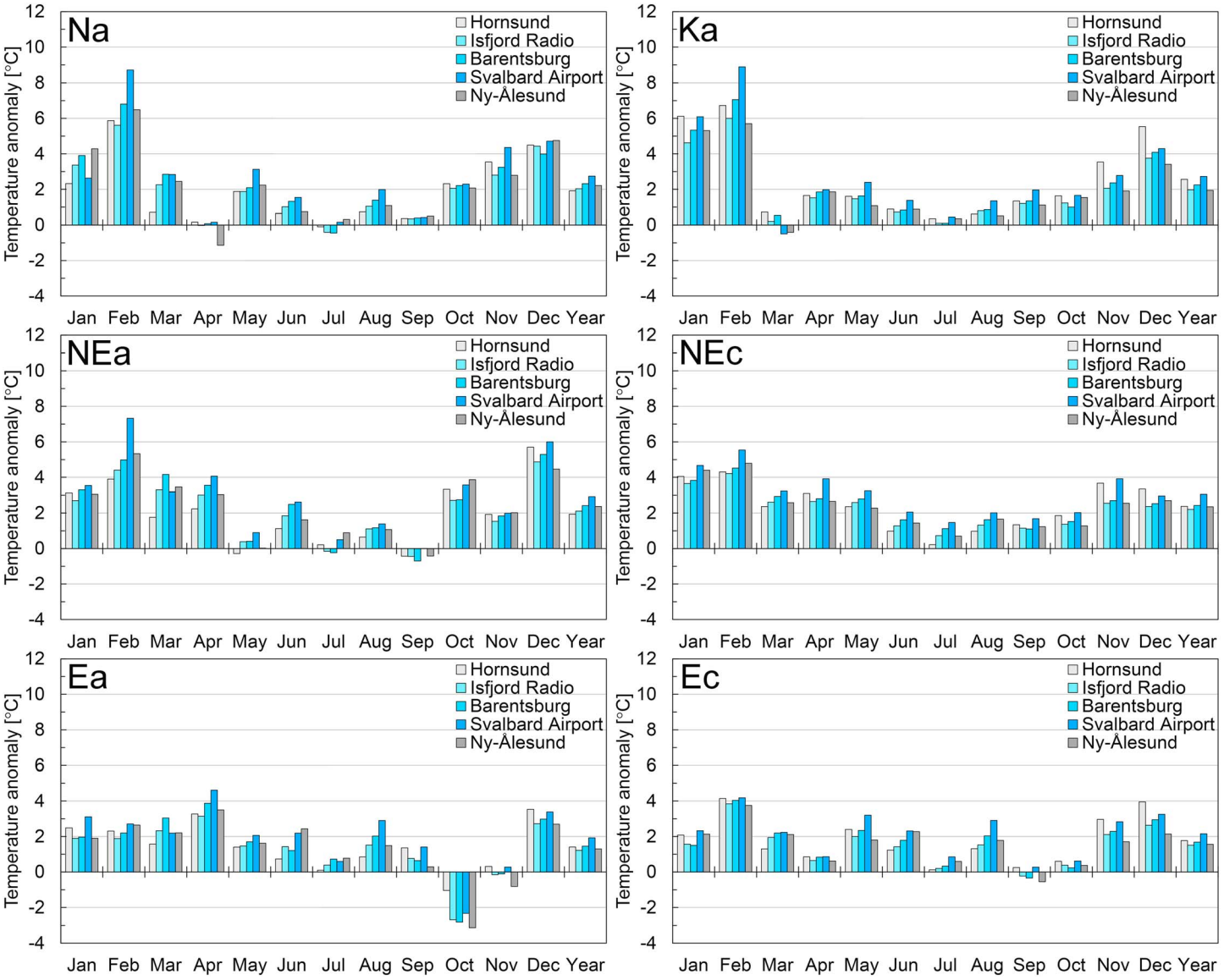

Figure 7. Monthly air temperature anomalies during the recent period 2001–2015 (with respect to the 1971–2000 mean) for the six AC types contributing most (in total ~80%) to the recent warming (cf. Figure 6).

3.5. Temperature Anomalies Caused by Changes in Atmospheric Circulation (AC) and Air Mass Characteristics

Figure 6 suggests that a large part of the recent warming is linked to a few AC types. As mentioned in section 1, the major questions are as follows: (RQ1) How much of the recent warming is caused by changes in frequencies of AC types and (RQ2) how much of the recent warming is caused by changes in air mass characteristics for different AC types? To elucidate RQ1, we have applied the 1971–2000 mean temperature for each AC type (Figure 4) but used frequencies of AC types for the recent period 2001–2015. The calculations are made by using formula (1), cf. section 2. The monthly anomalies based on the cumulative sum of individual contributions for all AC types are shown in Figure 9a.

Compared to the real observed temperature anomalies (transparent colors in Figure 9a), the results indicate that changes in AC have played a minor role on the total recent surface warming. On an annual basis changes in AC contributed approximately 10% to the total recent warming. However, in winter (December-January-February, DJF) the contribution was larger, approximately 25%. The results also show

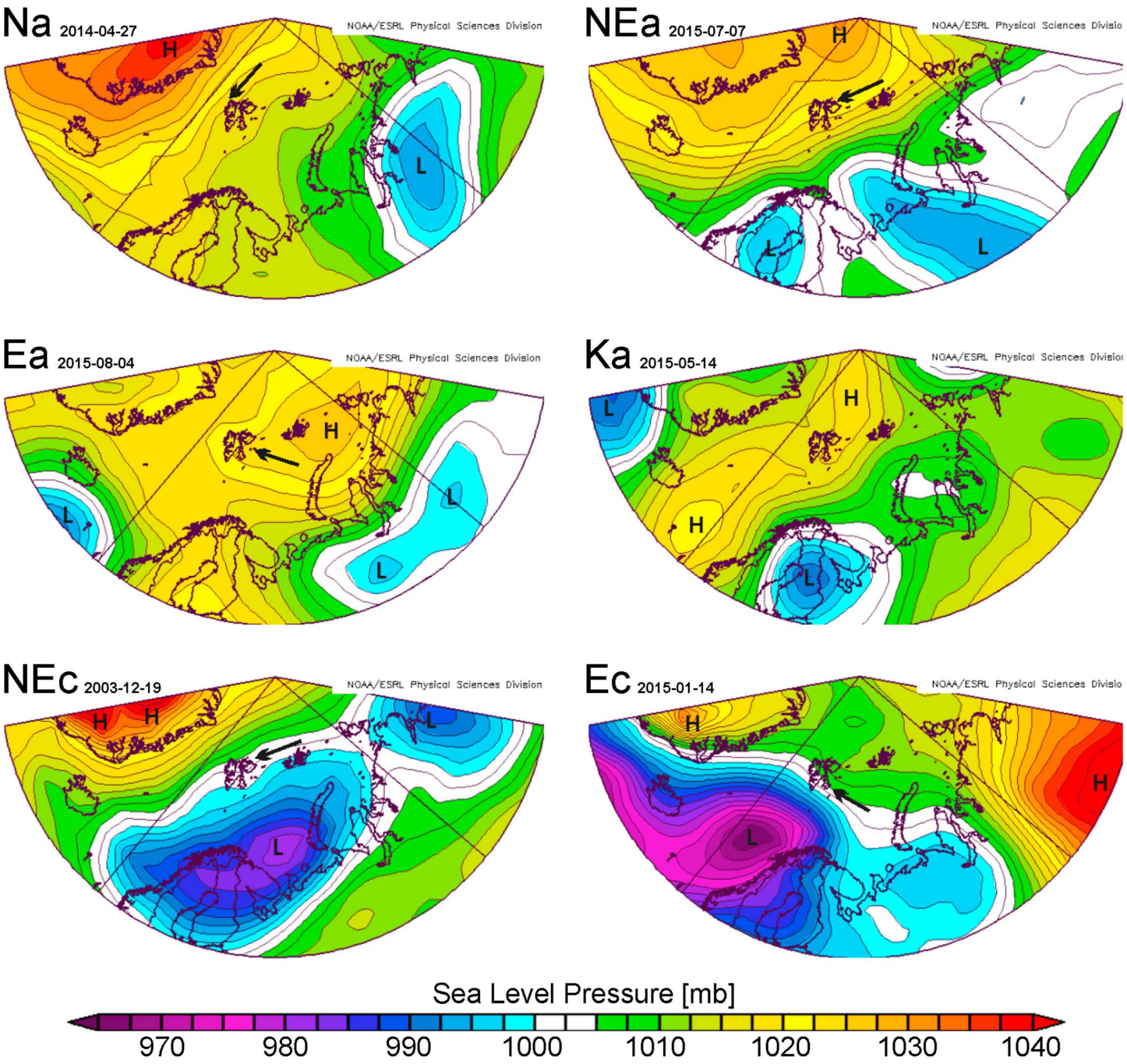

Figure 8. Example of typical sea level pressure (SLP) pattern from NCEP/NCAR Reanalysis for the six AC types contributing most to the recent warming over Spitsbergen. The arrow shows direction of air advection. Images were provided by the NOAA/ESRL Physical Sciences Division, Boulder, Colorado, from their Web site at http://www.esrl.noaa.gov/psd/.

that changes just in AC would contribute negatively in several months, especially in March, and also during May to October.

To elucidate RQ2, the mean temperatures for each AC type during 2001–2015 are allocated to the frequency distribution of AC types during 1971–2000. The resulting monthly anomalies calculated by formula (2) are shown in Figure 9b. The results indicate that a major part of the warming from 1971–2000 to 2001–2015 may be explained by higher temperatures in air masses for the different AC types. As indicated by Figure 9a, however, increased frequencies of "warm" AC types have a small contribution (~25%) to the winter

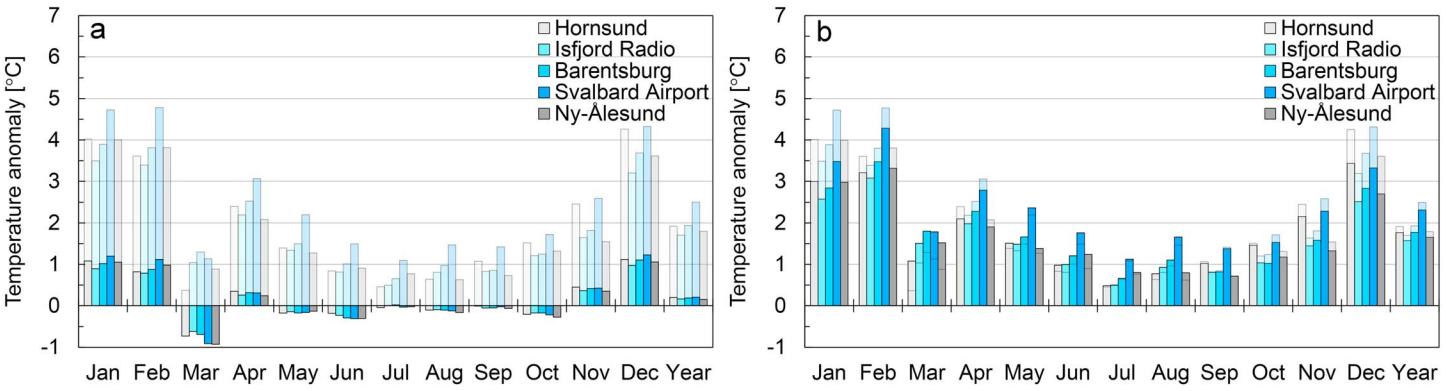

Figure 9. (a) Monthly and annual temperature anomalies for the recent period 2001–2015 (with respect to the 1971–2000 mean) derived from changes in AC only, cf. section 2, formula (1). Values are compared to the observed temperature anomalies (transparent colors) shown in Figure 2b. (b) Monthly and annual temperature anomalies for the recent period 2001–2015 (with respect to the 1971–2000 mean) derived from changes in air mass characteristics only, cf. section 2, formula (2).

warming. In March, higher temperatures in the AC-type distribution during 1971–2000 would have resulted in increased temperatures, but this effect is counteracted by increased frequencies of "cold" AC types.

3.6. Sea Ice Concentration (SIC) and Surface Air Temperature (SAT) at Spitsbergen in Relation to Atmospheric Circulation (AC) Types

The last major research question (RQ3) is related to the influence on the recent warming of changes in feedback effects caused by reduced SIC. The study was performed using ice observation both on regional scale

Table 2. Interactions Between Regional SIC (Predictors) and SAT at Svalbard Airport (Predictand) for Specific AC Types and Seasons Winter (DJF), Spring (MAM), Summer (JJA), and Autumn (SON)[a]

Season	AC Type	No. of Cases	*R*	Ice Region	RMSE (deg)
Winter December–February	Na	44	0.84	2, 3, 4	3.4
	NEa	77	0.79	3, 1	4.1
	Ea	100	0.67	3, 5	4.1
	Ka	92	0.78	5, 2	4.6
	NEc	199	0.74	3, 2, 1, 4	4.4
	Ec	259	0.62	3, 4, 1	4.6
	The other types	937	0.59	3, 1, 2, 4	5.6
Spring March–May	Na	101	0.73	3, 2, 5	5.1
	NEa	139	0.74	3, 2, 1, 5	4.9
	Ea	148	0.70	3, 2, 1	4.6
	Ka	179	0.72	3, 2, 5	5.6
	NEc	133	0.77	3, 2, 5	5.1
	Ec	174	0.64	3, 2, 4	5.4
	The other types	867	0.66	3, 2, 4, 5	4.7
Summer June–August	Na	73	0.62	4, 2	2.5
	NEa	55	0.76	3, 2, 1	1.9
	Ea	79	0.58	3, 2, 1, 4	2.5
	Ka	283	0.58	3, 4, 1, 2	1.9
	NEc	70	0.66	4	1.8
	Ec	91	0.50	3, 1, 5	2.4
	The other types	1090	0.52	4, 3, 2, 1	2.2
Autumn September–November	Na	57	0.75	4, 1	3.9
	NEa	79	0.83	4, 1, 2	3.4
	Ea	64	0.78	4, 1, 3	3.3
	Ka	156	0.78	4, 3	4.1
	NEc	171	0.70	4, 5	4.0
	Ec	170	0.67	4, 5	3.9
	The other types	1025	0.62	4, 1, 2	4.4

[a]The regions are those shown in Figure 1c. The data period is 1992–2010, but ice information was available only for certain days in the period. RMSE is the root-mean-square error, and R^2 is the coefficient of determination.

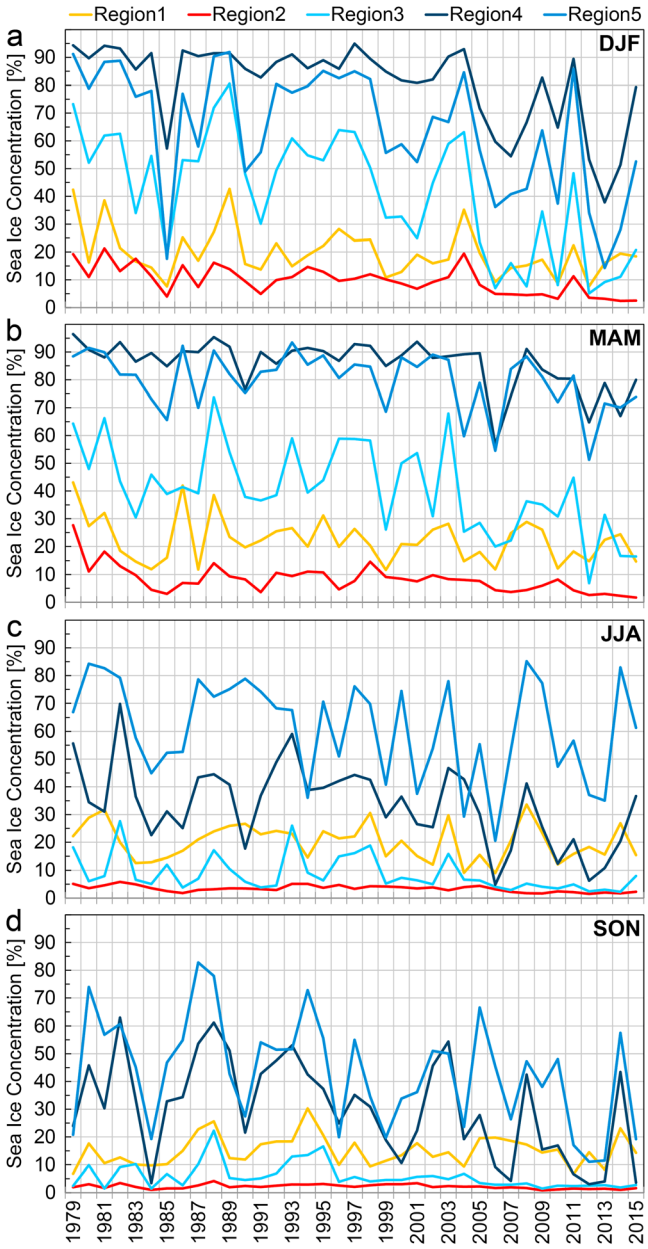

Figure 10. Mean seasonal regional SIC between 1979 and 2015 for the five regions defined in Figure 1c.

and on local scale. The regional scale comprises five sea areas around Spitsbergen (Figure 1c), whereas the local scale comprises point observations near the weather stations on Spitsbergen (Figure 1d).

3.6.1. Interactions Between Sea Ice Concentration (SIC) and Surface Air Temperature (SAT) on Regional Scale

The influence of temperature on air flow from the different ice regions was tested by stepwise regression analysis for the period 1992–2010, cf. section 2. Each SIC observation was related to the actual AC type. Of particular interest were those AC types that had contributed most to the recent temperature increase on Spitsbergen, cf. Figures 6 and 7, Na, NEa, Ea, Ka, NEc, and Ec. For brevity only these are shown explicitly in Table 2.

Region No. 3, situated to the southeast of Spitsbergen, seemed to be the region of largest influence on air temperature in winter, spring, and summer (Table 2). During autumn region 4, which is situated to the east of Spitsbergen, was of greater importance. The percentage of autumn SIC in region 4 varied from near 0 to more than 60, whereas region 3 was mostly free from ice (Figure 10) and did not contribute as a predictor for SAT.

In region 3 a remarkable shift in SIC took place in 2005 and 2004 in spring and winter, respectively, when a significant reduction in the ice cover was observed (Figure 10). A corresponding shift in SIC was also seen in regions 4 and 5 in winter.

The highest regression correlation coefficients (R), about 0.8, were obtained for the anticyclonic AC types: Na, NEa, and Ka during winter and for type NEa during autumn. This means that for those cases two thirds of the variance was accounted for by the regression. In general, the AC types that had contributed to the largest temperature anomalies (cf. Figures 6 and 7) were more strongly linked to SIC than those in the control group: "the other types"; see Table 2. Similar results to those for Svalbard Airport were also seen for the other stations on Spitsbergen, i.e., Ny-Ålesund, Isfjord Radio, Barentsburg, and Hornsund (not shown).

3.6.2. Interactions Between SIC and SAT on Local Scale

With local SIC as the only predictor a temperature regression for all stations and for the same AC types and seasons as shown in Table 2 was performed for the period 1975–2015. Compared with the results for the regional SIC, R was now much lower, with very few exceptions higher than 0.5 (not shown). This implies that the variance accounted for by the regression was mostly less than one fourth, whereas when regional SIC was used as predictor, two thirds of the variance was accounted for in some cases. This

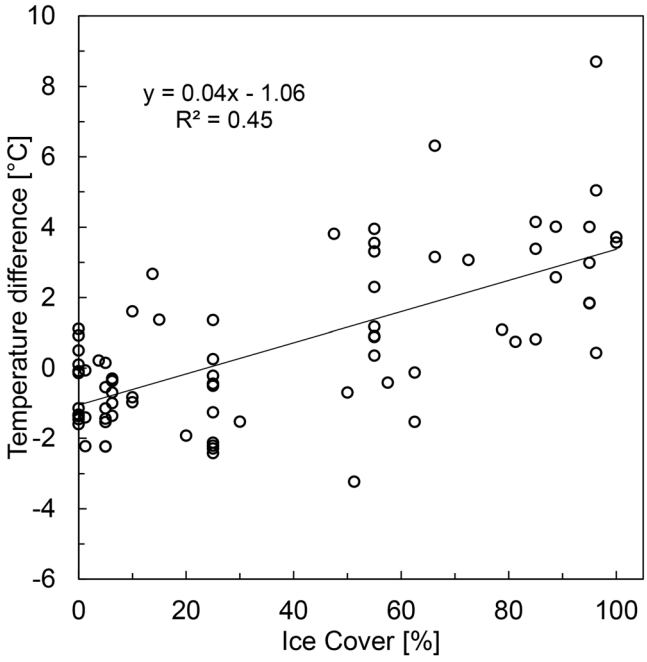

Figure 11. Temperature difference between the stations Janssonhaugen and Svalbard Airport in relation to local SIC (%) on Isfjorden outside Svalbard Airport for AC types Ca and Ka. The data period is December 2000 to December 2015 during the season December–April.

suggests that the temperature observed on the land stations at Spitsbergen is less influenced by the local SIC than by the regional SIC.

Nevertheless, for particular AC types, local SIC was found to have a paramount influence on occurrence of surface inversions. Situations with surface inversions occurred particularly under AC types Ca and Ka, i.e., high pressure with calm or no wind. The temperature difference between the stations Janssonhaugen (270 m asl) and Svalbard Airport (28 m asl) was taken as a measure for the inversion in Isfjorden. During these cold weather situations, energy from an open fjord jeopardized formation of the surface inversion, whereas the inversion could develop over an ice-/snow-covered fjord (Figure 11). By linear regression R was found to be 0.67, which implies that local SIC may account for nearly half of the variance in temperature differences between the two stations. For an open fjord the temperature difference between Janssonhaugen and Svalbard Airport was −1.1°C according to the regression line, whereas with an ice-covered fjord the difference was to 3.3°C.

If there has been a trend in the SIC of Isfjorden, then there should also be a trend in the temperature difference between a high-level station like Janssonhaugen and a low-level station like Svalbard Airport. The trend in SIC might be somewhat uncertain as the observations of SIC are not daily. Moreover, there is also a trend toward larger SIC from December to the end of April, which might bias the seasonal mean value if there are different numbers of observations within each month. We tried to overcome this by taking the average SIC for each month and then taking the mean of the means for the 5 months in the December–April season (Figure 12). However, from 1997 the assessment of SIC is considered to be accurate, since it is based on 15–20 observations per month, whereas at the start, in 1975, it was more uncertain, being based on only five observations within each month. Before 1992 the differences between the local SIC series are larger than in the most recent part of the series, so probably, this might also be attributed to the uncertainty of the data.

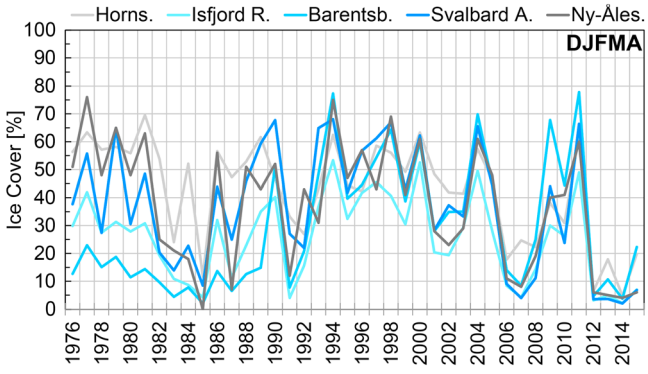

Figure 12. Average SIC (%) outside the meteorological stations (cf. Figure 1d) on Spitsbergen for the season December–April (DJFMA).

4. Discussion

4.1. Temperature Anomalies Caused by Changes in AC and Air Mass Characteristics

Our analyses show that for all AC patterns there has been a substantial warming in western Spitsbergen from the normal period 1971–2000 to the recent period 2001–2015 (Figure 5). Moreover, our results suggest that changes in frequencies of AC types have a minor role in the total surface warming recorded since 2001 (Figure 9a). This means that the situation has changed

compared to the warming from 1960 to the 1990s that was strongly related to changing frequencies of circulation patterns [*Hanssen-Bauer and Førland*, 1998]. Although we found that changes in AC contributed to the winter warming by approximately 25%, it contributed negatively in several months, especially in March, and also during May to October. However, this leads to an annual contribution to the recent warming of only 10% or so. The smaller increase in temperature in March compared to February and April (Figure 2) can at least partly be explained by changed AC in between the two periods.

Several of the recent warmest ever winters at Svalbard Airport were characterized by average or even low Arctic Oscillation (AO) mode [*Nordli et al*., 2014]. *Hanssen-Bauer and Førland* [1998] emphasized that although the warming from the 1960s to the 1990s was related to changes in atmospheric circulation, variations in circulation pattern accounted for only a fraction of the temperature increase at Svalbard Airport from 1912 to the 1930s and for the temperature decrease from the 1930s to the 1960s. They stressed that other predictors (SST, SIC, and cloudiness) were needed to model long-term temperature variability. *Maslanik et al*. [2007] argued that there might be more regional, sea level pressure (SLP) patterns that contribute significantly to interannual variability in SIC and SAT.

The results presented in this study suggest that most of the recent warming may be attributed to changes in air mass characteristics and a smaller part (~10%) to changes in frequencies of the AC types (cf. Figure 9). However, as much as ~80% of the recent warming is accounted for by only six AC types: Na, NEa, Ea, Ka, NEc, and Ec (Figure 6).

4.2. Reasons for Changes in Air Mass Characteristics for AC Types

The results discussed in the previous section indicate that most of the recent warming at Spitsbergen can be attributed to changes in air mass characteristics. The reasons for warming of air masses may be the following: (1) local effects of reduced wintertime ice cover on the fjords outside the stations, (2) regional influence of reduced sea ice in the seas surrounding Spitsbergen, (3) regional influence of increased sea surface temperatures, and (4) other mechanisms for large-scale Arctic warming.

4.2.1. Local Effects of Reduced Wintertime SIC on the Fjords Outside the Stations

The local SIC on Isfjorden near Svalbard Airport has decreased significantly during the last two decades (Figure 12). Least squares regression indicates that during the period 1997–2015, where the SIC data are accurate, the SIC has been reduced from 58% coverage to 6% coverage. The average SIC for our recent period of investigation 2001–2015 is 26%, whereas the coverage for the period 1976–2000 was 43%. Since 1997, all three fjords had two periods with low SIC (Figure 12). For the periods 2006–2008 and 2012–2015 all five sites respond in a similar way. This is in line with results by *Muckenhuber et al*. [2016] which suggest that such long-lasting periods involves an oceanic mechanism. This is also supported by *Nilsen et al*. [2016] who argue that recent changes in AC patterns have brought warm Atlantic water (AW) from the West Spitsbergen Current onto the West Spitsbergen Shelf (WSS) and into the fjords even during winter [*Cottier et al*., 2007; *Nilsen et al*., 2008; *Pavlov et al*., 2013]. Since atmospheric forcing of the WSS is strongest during the winter months, the intrusion of AW is often largest during these months and plays a decisive role for the sea ice cover in fjords and shelf areas [*Nilsen et al*., 2016].

Ice coverage favors inversion buildups, so more open water may be important for local climate. We have seen that this is of particular importance in high-pressure situations, which are characterized by almost calm air captured in the fjord basin of Isfjorden (Figure 11). Therefore, changes in SIC could well be the reason that Svalbard Airport has warmed more than the other stations on Spitsbergen as found in this article and also by *Gjelten et al*. [2016]. When the fjord is open during winter, there is an energy transfer from the fjord water to the air that leads to convection in the air mass, and the temperature gradient will be negative. For an ice-covered fjord (and in particular for snow-covered ice) much of this energy transfer is reduced so that surface inversion can be built up.

For other AC types, however, our results showed that the temperature observed on the land stations at Spitsbergen was less influenced by the local SIC than by the regional SIC.

4.2.2. Regional Influence of Reduced SIC in the Seas Surrounding Spitsbergen

The sea ice cover increases the surface albedo and insulates the ocean from heat loss to the atmosphere. Regional climate changes affect the sea ice characteristics that can feed back on the climate system, both regionally and globally [*Vaughan et al*., 2013]. In the Arctic Ocean the sea ice loss has been largest during summer [*Comiso*, 2012]. In contrast, the SIC north of Svalbard has experienced a larger decline during winter

since 1979 [*Onarheim et al*., 2014]. This is also supported by our analyses related to the regional ice cover in region 5 (Figure 10). Compared to the other seasons, the most dramatic ice loss near Svalbard has occurred in winter, whereas around the peak of the ice season, spring, changes are less and in summer no trend is seen in that region.

Previous studies have suggested that the land temperature on Svalbard is sensitive to the location of the regional ice edge [e.g., *Benestad et al*., 2002]. This is in line with what is found here. The regions with the largest reduction of SIC had the greatest influence on land surface temperature, and the influence from the regional SIC was greater than from local SIC. As shown in Figure 1a there is a large gradient in the recent temperature anomaly from southwestern to northeastern parts of the Svalbard region. The same pattern is also found in temperature projections for Svalbard up to year 2100 [*Førland et al*., 2011]. The temperature anomaly pattern coincides with the recent decrease in winter sea ice extent in the Barents Sea, which is the most pronounced sea ice decline in the Arctic [*Parkinson and Cavalieri*, 2008; *Årthun et al*., 2012]. The sea ice loss in the Barents Sea is primarily forced by winter ocean heat fluxes [e.g., *Dmitrenko et al*., 2014; *Polyakov et al*., 2010]. During its passage through the Barents Sea, the Atlantic water loses most of its heat to the atmosphere [*Häkkinen and Cavalieri*, 1989; *Årthun and Schrum*, 2010]. In our study a corresponding decrease is found in region 3 (southeast of Spitsbergen) and region 4 (east of Spitsbergen) during winter and spring since 2005 (Figure 10). Especially, region 3 seemed to be the region of largest influence on air temperature in winter and spring (cf. Table 2). As shown in Figure 6, the greatest contribution to the recent warming is associated with wintertime situations of cyclonic air advection from northeast-east (NEc and Ec), related to low-pressure system moving into the Barents Sea (Figure 8). Thus, the reduced SIC found in especially regions 3–5 with corresponding high regression correlations to especially specific anticyclonic AC types in winter suggests that at least part of the atmospheric warming observed in Spitsbergen is driven by heat exchange from declining sea ice in the Barents Sea and the region north of Svalbard.

4.2.3. Regional Influence of Increased Sea Surface Temperatures (SSTs)

SSTs have increased in most of the Arctic's marginal seas [e.g., *Timmermans and Proshutinsky*, 2015]. Below the surface, pulses of increasingly warmer Atlantic water, entering the Arctic through Fram Strait and through the Barents Sea, have been documented by, e.g., *Dmitrenko et al*. [2014] and *Carmack et al*. [2015].

According to *Onarheim et al*. [2014], the ice edge north of Svalbard has retreated toward the northeast, along the AW pathway. Between 1979 and 2012, an overall AW warming of 1.1°C was observed in this region. During the same period the regional winter air temperature increased by 6.9°C [*Onarheim et al*., 2014] based on ERA-Interim reanalysis [*Dee et al*., 2011].

4.2.4. Other Mechanisms for Large-Scale Arctic Warming

As stated in section 1 and discussed above, several factors may contribute to the large-scale Arctic warming. According to *Bindoff et al*. [2013], it is likely that there has been an anthropogenic contribution to the very substantial Arctic warming over the past 50 years. *Fyfe et al*. [2013] conclude that the combined surface response to rising black carbon aerosol emissions, recovery from the eruption of Santa Maria (1902), and transition of the Atlantic Multidecadal Oscillation (AMO) to its positive phase was a positive contribution in the period before 1939, while natural variability opposed the emerging greenhouse gas (GHG) contribution during the period 1939–1970. Arctic average surface warming from 1970 to 2005 was dominated by GHG warming with a smaller contribution from the transition of the AMO to its positive phase [*Fyfe et al*., 2013]. A new study by *Navarro et al*. [2016] shows that the sulfate aerosol reductions in Europe since 1980 can potentially explain a significant fraction of Arctic warming over that period. Contrary to a widespread assumption, *Pithan and Mauritsen* [2014] conclude that temperature feedbacks are the most important contributors to Arctic amplification in contemporary climate models, while the surface albedo feedback is the second main contributor. A recent study by *Johannessen et al*. [2016] concludes that the Arctic amplification is stronger during the early twentieth century warming than that for the recent years because of the increased global warming background upon which amplified Arctic warming is superimposed.

While SAT in the Arctic has increased at approximately twice the global rate in recent decades, the spatial and temporal variability is also large. In January–April 2016 extensive regions of Arctic temperature extremes were observed and related to midlatitude atmospheric circulation and large-scale AC patterns [*Overland and Wang*, 2016]. Thus, the spatial variability in SAT is largely governed by the changes in large-scale AC patterns, which may either amplify or equalize the Arctic response of the global radiative forcing.

5. Conclusions

This study has examined the recent surface air temperature (SAT) anomalies (recent period 2001–2015 compared to the normal period 1971–2000) at five weather stations on western Spitsbergen and their relation to atmospheric circulation (AC) and sea ice concentration (SIC). Our conclusions are as follows:

1. For all seasons there has been a substantial warming in western Spitsbergen. Greatest SAT increase was observed in winter (DJF) with 3.4–4.6°C.
2. Significant warming is found for all AC patterns in all seasons. A major part of the warming can be attributed to changes in air mass characteristics and mainly linked to a few AC types. The greatest contribution to the recent warming is associated with situations of both cyclonic and anticyclonic air advection from north and east and situations with an anticyclonic ridge. In total, six AC types, which occur on average 41% of days in a year, contribute approximately 80% of the recent warming.
3. Changes in frequencies of atmospheric circulation have a minor role on the total recent surface warming and contribute approximately 10% annually and 25% in winter.
4. A highly significant relationship was found between the SAT at Spitsbergen weather stations and regional as well as local SIC.
5. The high correlation between SAT and SIC for air masses from east and north of Spitsbergen suggests that a major part of the atmospheric warming observed in Spitsbergen is driven by heat exchange from the larger open water areas in the Barents Sea and the region north of Spitsbergen.
6. The influence of SIC on SAT is also strong during periods with nonadvectional anticyclone ridge. Locally in the fjords, the calm winds in these situations enhance the influence of the local energy balance. Reduction of local SIC increases temperature near fjords more than on mountain plateaus. This effect seemed to be strongest in the fjord basin of Isfjorden. Thus, the recent decline in local SIC in Isfjorden is probably the main reason that Svalbard Airport has warmed more than the other stations on Spitsbergen.
7. Finally, the general warming seen for all AC types on Spitsbergen suggests additional contributions from large-scale mechanisms, such as the general background warming and higher sea surface temperatures.

Acknowledgments

The study is a part of the projects *AWAKE-2* (Arctic Climate System Study of Ocean, Sea Ice and Glaciers Interactions in Svalbard Area) financed by EEA Grants-Norway Grants (project PL12-0003) and *ISFJORDEN* (Past and present climate), financed by the Research Council of Norway (project 227027). NCEP Reanalysis [*Kalnay et al*., 1996] data were provided by the NOAA/ESRL Physical Sciences Division, Boulder Colorado (www.esrl.noaa.gov/psd/). The calendar of AC types (Niedźwiedź Classification) [*Niedźwiedź*, 2013] was created manually and is available on request. Data on sea ice concentration were provided by Istjenesten, MET Norway (http://polarview.met.no), and EUMETSAT OSI SAF (http://www.osi-saf.org). Air temperature data were provided by Norwegian Meteorological Institute and the Institute of Geophysics of the Polish Academy of Science and are available from http://eklima.met.no. Air temperature data from the weather station on Janssonhaugen were provided by the University Centre in Svalbard, UNIS (http://www.unis.no/). C. Harris and R. Benestad smoothed the English. Two anonymous reviewers gave constructive comments. The contribution of all persons and institutions mentioned is gratefully acknowledged.

References

Arctic Monitoring and Assessment Programme (2012), Arctic climate issues 2011: Changes in Arctic snow, water, ice and permafrost, SWIPA 2011 Overview Rep.

Årthun, M., and C. Schrum (2010), Ocean surface heat flux variability in the Barents Sea, *J. Mar. Syst.*, *83*(1–2), 88–98, doi:10.1016/j.jmarsys.2010.07.003.

Årthun, M., T. Eldevik, L. H. Smedsrud, Ø. Skagseth, and R. B. Ingvaldsen (2012), Quantifying the influence of Atlantic heat on Barents sea ice variability and retreat, *J. Clim.*, *25*(13), 4736–4743, doi:10.1175/JCLI-D-11-00466.1.

Benestad, R. E., E. J. Førland, and I. Hanssen-Bauer (2002), Empirically downscaled temperature scenarios for Svalbard, *Atmos. Sci. Lett.*, *3*(2–4), 71–93, doi:10.1006/asle.2002.0050.

Bindoff, N. L., et al. (2013), Detection and attribution of climate change: From global to regional, in *Climate Change 2013: The Physical Science Basis. Contribution of Working Group I to the Fifth Assessment Report of the Intergovernmental Panel on Climate Change*, edited by T. F. Stocker et al., Cambridge Univ. Press, Cambridge, U. K., and New York.

Brümmer, B., S. Thiemann, and A. Kirchgäßner (2000), A cyclone statistics for the Arctic based on European Centrere-analysis data, *Meteorol. Atmos. Phys.*, *75*(3–4), 233–250, doi:10.1007/s007030070006.

Carmack, E., et al. (2015), Toward quantifying the increasing role of oceanic heat in sea ice loss in the New Arctic, *Bull. Am. Meteorol. Soc.*, *96*(12), 2079–2105, doi:10.1175/BAMS-D-13-00177.1.

Cohen, J., et al. (2014), Recent Arctic amplification and extreme mid-latitude weather, *Nat. Geosci.*, *7*(9), 627–637.

Comiso, J. C. (2012), Large decadal decline of the arctic multiyear ice cover, *J. Clim.*, *25*(4), 1176–1193, doi:10.1175/JCLI-D-11-00113.1.

Cottier, F. R., F. Nilsen, M. E. Inall, S. Gerland, V. Tverberg, and H. Svendsen (2007), Wintertime warming of an Arctic shelf in response to large-scale atmospheric circulation, *Geophys. Res. Lett.*, *34*, L10607, doi:10.1029/2007GL029948.

Dee, D. P., et al. (2011), The ERA-Interim reanalysis: Configuration and performance of the data assimilation system, *Q. J. R. Meteorol. Soc.*, *137*(656), 553–597, doi:10.1002/qj.828.

Deser, C., J. E. Walsh, and M. S. Timlin (2000), Arctic sea ice variability in the context of recent atmospheric circulation trends, *J. Clim.*, *13*(3), 617–633, doi:10.1175/1520-0442(2000)013<0617:ASIVIT>2.0.CO;2.

Dmitrenko, I. A., et al. (2014), Heat loss from the Atlantic water layer in the northern Kara Sea: Causes and consequences, *Ocean Sci.*, *10*(4), 719–730, doi:10.5194/os-10-719-2014.

Førland, E. J., R. Benestad, I. Hanssen-Bauer, J. E. Haugen, and T. E. Skaugen (2011), Temperature and precipitation development at Svalbard 1900–2100, *Adv. Meteorol.*, *2011*, 1–14, doi:10.1155/2011/893790.

Førland, E., I. Hanssen-Bauer, and P. Nordli (1997), Climate statistics and long-term series of temperature and precipitation at Svalbard and Jan Mayen, DNMI Rep., 21(97), 43.

Fyfe, J. C., K. von Salzen, N. P. Gillett, V. K. Arora, G. M. Flato, and J. R. McConnell (2013), One hundred years of Arctic surface temperature variation due to anthropogenic influence, *Sci. Rep.*, *3*, 2645, doi:10.1038/srep02645.

Gjelten, H. M., Ø. Nordli, K. Isaksen, E. J. Førland, P. N. Sviashchennikov, P. Wyszynski, U. V. Prokhorova, R. Przybylak, B. V. Ivanov, and A. V. Urazgildeeva (2016), Air temperature variations and gradients along the coast and fjords of western Spitsbergen, *Polar Res.*, *35*, doi:10.3402/polar.v35.29878.

Graversen, R. G., P. L. Langen, and T. Mauritsen (2014), Polar amplification in CCSM4: Contributions from the lapse rate and surface albedo feedbacks, *J. Clim.*, *27*(12), 4433–4450, doi:10.1175/JCLI-D-13-00551.1.
Häkkinen, S., and D. J. Cavalieri (1989), A study of oceanic surface heat fluxes in the Greenland, Norwegian, and Barents Seas, *J. Geophys. Res.*, *94*, 6145–6157, doi:10.1029/JC094iC05p06145.
Hanssen-Bauer, I. (2002), Temperature and precipitation in Svalbard 1912–2050: Measurements and scenarios, *Polar Rec.*, *38*(206), 225–232, doi:10.1017/S0032247400017757.
Hanssen-Bauer, I., and E. J. Førland (1998), Long-term trends in precipitation and temperature in the Norwegian Arctic: Can they be explained by changes in atmospheric circulation patterns?, *Clim. Res.*, *10*(2), 143–153.
Hughes, N. E., and P. Wagner (2015), Knowledge and forecasts of sea ice extent and icebergs—"Barents Sea SE" and "Jan Mayen", doi:10.13140/RG.2.1.5003.6562.
Isaksen, K., J. L. Sollid, P. Holmlund, and C. Harris (2007), Recent warming of mountain permafrost in Svalbard and Scandinavia, *J. Geophys. Res.*, *112*, F02S04, doi:10.1029/2006JF000522.
Jaiser, R., K. Dethloff, D. Handorf, A. Rinke, and J. Cohen (2012), Impact of sea ice cover changes on the Northern Hemisphere atmospheric winter circulation, *Tellus A*, *64*, doi:10.3402/tellusa.v64i0.11595.
Johannessen, O., S. Kuzmina, L. Bobylev, and M. Miles (2016), Surface air temperature variability and trends in the Arctic: New amplification assessment and regionalisation, *Tellus A*, *68*, doi:10.3402/tellusa.v68.28234.
Kalnay, E., et al. (1996), The NCEP/NCAR 40-year reanalysis project, *Bull. Am. Meteorol. Soc.*, *77*(3), 437–471, doi:10.1175/1520-0477(1996)077<0437:TNYRP>2.0.CO;2.
Kwok, R., and D. A. Rothrock (2009), Decline in Arctic sea ice thickness from submarine and ICESat records: 1958–2008—Arctic sea ice thickness, *Geophys. Res. Lett.*, *36*, L15501, doi:10.1029/2009GL039035.
Lamb, H. H. (1972), British Isles weather types and a register of the daily sequence of circulation patterns 1861–1971, Her Majesty's stationery office.
Lindsay, R. W., J. Zhang, A. Schweiger, M. Steele, and H. Stern (2009), Arctic sea ice retreat in 2007 follows thinning trend, *J. Clim.*, *22*(1), 165–176, doi:10.1175/2008JCLI2521.1.
Lupikasza, E., and T. Niedźwiedź (2013), Frequency of ice days at selected meteorological stations in Svalbard, *Bull. Geogr. Phys. Geogr. Ser.*, *6*(1), doi:10.2478/bgeo-2013-0005.
Lupikasza, E., L. Malarzewski, T. Niedźwiedź, and K. Dobrowolska (2014), Trendy temperatury powietrza oraz liczby dni mroźnych iz przejściem temperatury przez w Arktyce Atlantyckiej i Syberyjskiej, *Problemy Klimatologii Polarnej*, *24*, 5–24.
Marsz, A. A., and A. Styszynska (2013), *Climate and Climate Change at Hornsund*, Gdynia Maritime Univ, Svalbard.
Maslanik, J., S. Drobot, C. Fowler, W. Emery, and R. Barry (2007), On the Arctic climate paradox and the continuing role of atmospheric circulation in affecting sea ice conditions, *Geophys. Res. Lett.*, *34*, L03711, doi:10.1029/2006GL028269.
Muckenhuber, S., F. Nilsen, A. Korosov, and S. Sandven (2016), Sea ice cover in Isfjorden and Hornsund, Svalbard (2000–2014) from remote sensing data, *Cryosphere*, *10*(1), 149–158, doi:10.5194/tc-10-149-2016.
Navarro, J. C., V. Varma, I. Riipinen, O. Seland, A. Kirkevag, H. Struthers, T. Iversen, H.-C. Hansson, and A. M. L. Ekman (2016), Amplification of Arctic warming by past air pollution reductions in Europe, *Nat. Geosci.*, *9*(4), 277–281.
Niedźwiedź, T. (1993), The main factors forming the climate of the Hornsund [Spitsbergen], in *Zeszyty Naukowe Uniwersytetu Jagiellońskiego. Prace Geograficzne*, pp. 49–63, Institute of Geography and Spatial Management of the Jagiellonian Univ., Kraków, Poland.
Niedźwiedź, T. (2003), Współczesna zmienność cyrkulacji atmosfery, temperatury powietrza i opadów atmosferycznych na Spitsbergenie, *Problemy Klimatologii Polarnej*, *13*, 79–92.
Niedźwiedź, T. (2013), The atmospheric circulation, in *Climate and Climate Change at Hornsund, Svalbard*, edited by A. A. Marsz and A. Styszyńska, pp. 57–74, Gdynia Maritime Univ., Gdynia, Poland.
Nilsen, F., F. Cottier, R. Skogseth, and S. Mattsson (2008), Fjord–shelf exchanges controlled by ice and brine production: The interannual variation of Atlantic Water in Isfjorden, Svalbard, *Cont. Shelf Res.*, *28*(14), 1838–1853, doi:10.1016/j.csr.2008.04.015.
Nilsen, F., R. Skogseth, J. Vaardal-Lunde, and M. Inall (2016), A simple shelf circulation model: Intrusion of Atlantic Water on the West Spitsbergen Shelf, *J. Phys. Oceanogr.*, *46*(4), 1209–1230, doi:10.1175/JPO-D-15-0058.1.
Nordli, Ø., R. Przybylak, A. Ogilvie, and K. Isaksen (2014), Long-term temperature trends and variability on Spitsbergen: The extended Svalbard Airport temperature series, 1898–2012, *Polar Res.*, *33*, doi:10.3402/polar.v33.21349.
Onarheim, I. H., L. H. Smedsrud, R. B. Ingvaldsen, and F. Nilsen (2014), Loss of sea ice during winter north of Svalbard, *Tellus A*, *66*, doi:10.3402/tellusa.v66.23933.
Overland, J. E., and M. C. Serreze (2012), Advances in Arctic atmospheric research, in *Arctic Climate Change: The ACSYS Decade and Beyond*, edited by P. Lemke and H.-W. Jacobi, pp. 11–26, Springer, Dordrecht, Netherlands.
Overland, J. E., and M. Wang (2010), Large-scale atmospheric circulation changes are associated with the recent loss of Arctic sea ice, *Tellus A*, *62*(1), 1–9, doi:10.1111/j.1600-0870.2009.00421.x.
Overland, J. E., and M. Wang (2016), Recent extreme arctic temperatures are due to a Split Polar Vortex, *J. Clim.*, doi:10.1175/JCLI-D-16-0320.1.
Overland, J. E., M. Wang, and S. Salo (2008), The recent Arctic warm period, *Tellus A*, *60*(4), 589–597, doi:10.1111/j.1600-0870.2008.00327.x.
Overland, J. E., J. A. Francis, E. Hanna, and M. Wang (2012), The recent shift in early summer Arctic atmospheric circulation, *Geophys. Res. Lett.*, *39*, L19804, doi:10.1029/2012GL053268.
Overland, J., K. Wood, and M. Wang (2011), Warm Arctic-cold continents: Climate impacts of the newly open Arctic Sea, *Polar Res.*, *30*, doi:10.3402/polar.v30i0.15787.
Park, D.-S. R., S. Lee, and S. B. Feldstein (2015), Attribution of the recent winter sea ice decline over the Atlantic sector of the arctic ocean, *J. Clim.*, *28*(10), 4027–4033, doi:10.1175/JCLI-D-15-0042.1.
Parkinson, C. L., and D. J. Cavalieri (2008), Arctic sea ice variability and trends, 1979–2006, *J. Geophys. Res.*, *113*, C07003, doi:10.1029/2007JC004558.
Pavlov, A. K., V. Tverberg, B. V. Ivanov, F. Nilsen, S. Falk-Petersen, and M. A. Granskog (2013), Warming of Atlantic Water in two west Spitsbergen fjords over the last century (1912–2009), *Polar Res.*, *32*, doi:10.3402/polar.v32i0.11206.
Pithan, F., and T. Mauritsen (2014), Arctic amplification dominated by temperature feedbacks in contemporary climate models, *Nat. Geosci.*, *7*(3), 181–184.
Polyakov, I. V., et al. (2010), Arctic ocean warming contributes to reduced polar ice cap, *J. Phys. Oceanogr.*, *40*(12), 2743–2756, doi:10.1175/2010JPO4339.1.
Przybylak, R. (2007), Recent air-temperature changes in the Arctic, *Ann. Glaciol.*, *46*(1), 316–324, doi:10.3189/172756407782871666.
Serreze, M. C., A. P. Barrett, and J. J. Cassano (2011), Circulation and surface controls on the lower tropospheric air temperature field of the Arctic, *J. Geophys. Res.*, *116*, D07104, doi:10.1029/2010JD015127.

Timmermans, M. -L., and A. Proshutinsky (2015), Sea surface temperature [in Arctic Report Card 2015]. [Available at http://www.arctic.noaa.gov/reportcard.]

Tonboe, R. T., S. Eastwood, T. Lavergne, A. M. Sørensen, N. Rathmann, G. Dybkjær, L. T. Pedersen, J. L. Høyer, and S. Kern (2016), The EUMETSAT sea ice concentration climate data record, *The Cryosphere*, *10*(5), 2275–2290, doi:10.5194/tc-10-2275-2016.

Vaughan, D. G., et al. (2013), Observations: Cryosphere, in *Climate Change 2013: The Physical Science Basis. Contribution of Working Group I to the Fifth Assessment Report of the Intergovernmental Panel on Climate Change*, edited by T. F. Stocker et al., Cambridge Univ. Press, Cambridge, U. K., and New York.

Walczowski, W. (2013), Frontal structures in the West Spitsbergen Current margins, *Ocean Sci.*, *9*(6), 957–975, doi:10.5194/os-9-957-2013.

World Meteorological Organization (2011), CLIMATE NORMALS, CCl/MG/2011/Doc.10, ITEM 10, World Meteorological Organization, Denver, Colo.